DYNAMIC ANALYSIS OF OVERHEAD CABLE VIBRATIONS AS A RESULT OF ICE SHEDDING

László E. KOLLÁR, Masoud FARZANEH
NSERC/Hydro-Quebec/UQAC Industrial Chair on Atmospheric Icing of Power Network Equipment (CIGELE) and Canada Research Chair on Atmospheric Icing Engineering of Power Networks (INGIVRE) at the University of Quebec at Chicoutimi – 555 Boul. de l'Université, Chicoutimi, Quebec G7H 2B1 – Canada
laszlo_kollar@uqac.ca

Abstract

The dynamic behavior of overhead transmission line cables caused by ice shedding was examined numerically and is described in this paper. The finite element analysis software ADINA is used to develop models of the ice-covered cable and the suspension structure. Static analysis of overhead cables with ice loads and dynamic analysis of their vibration as a result of ice shedding are carried out, and results are compared to former experimental observations made on a five-span section. A two-span model is also developed and vibrations are simulated after ice sheds from one span. Two criteria for ice failure are applied and thereby the model may be used to predict if ice on the other span breaks, due to resulting vibrations.

INTRODUCTION

Overhead transmission lines are subject to various types of loads. Most of them may be considered as static loads, like steady wind, ice accretion, temperature change, or maintenance and construction procedures, but some of them must be treated as dynamic loads, e.g. wind-induced vibrations, ice shedding, forces due to flashovers, forces due to mechanical de-icing processes, or exceptional events such as conductor breakage, tower collapse, or drop of conductor suspension assembly.
Ice shedding on transmission lines may result in high-amplitude vibrations and excessive transient dynamic forces at the suspension structure, thereby leading to two categories of problems. High-amplitude vibrations may cause flashover between adjacent cables, while excessive forces at the suspension may break the insulator or, in extreme cases, damage the tower. Therefore, it is important to predict the maximum jump height of the unloaded span and the maximum drop in the span that remains loaded, as well as the maximum cable tension and the maximum swinging of the insulator string which occurs during the oscillation of the cable. These vibrations can also break the ice on the loaded spans depending on the ice properties, thereby removing ice from additional spans. However, the additional ice shedding initiated may further amplify vibrations to the point of damaging some of the line members.
The first studies on ice shedding were concerned with the maximum jump height of the cable following sudden ice release. A series of load-dropping tests performed on a five-span section was reported in [1]. Authors presented a simple method to calculate the jump height, and compared calculated values to experimental results. A finite element model was developed in [2], which is applicable to study both the static and dynamic effects of ice shedding on overhead transmission lines. They simulated the loads applied to the towers and cable motion caused by ice shedding, and performed experiments in order to validate numerical results. A similar finite element model was constructed in [3], where several ice-shedding scenarios were simulated with investigating the effects of different parameters such as ice thickness, span length, difference in elevation between end and suspension points, number of spans per line section, presence of unequal spans and partial ice

shedding on sub-spans. The finite element method was also used in [4] in order to develop two- and four-span models and explain a transmission line failure due to ice-shedding effects.
The models listed in the previous paragraph do not distinguish the behavior of cable and ice, which is due to different material properties; they assume only different densities of the bare and iced cables. The objective of the present paper is to provide a simple method for considering ice properties when modeling iced cable vibrations caused by ice shedding on the adjacent span, which makes it possible to predict ice breaking even if the cable is not damaged. Moreover, an attempt is made to model the effect of vibration on the suspension structure. In order to achieve this goal, finite element models of the iced cable and the suspension structure are constructed, and different ice shedding scenarios are simulated in this study. The reliability of the models is tested by comparing simulation results to former experimental observations [1], made on a five-span section where the middle span was loaded, and then the ice load was suddenly released. Further ice shedding scenarios are modelled by applying a two-span model, and the dynamic effects of the resulting vibrations on the ice and the suspension structure are examined. Ice is not considered as a distinct material; however, two failure criteria for ice are defined, which provides approximate information if ice breaking occurs during the oscillation. The improvement of these criteria and the decision about ice failure are subjects of future research. A finite element model, with built-in material properties of ice, is developed in a parallel study [5].

MODELING APPROACH

Models of the iced cable and suspension structure are constructed using the finite element analysis software ADINA [6]. The modeling approach is based on that introduced in [2] and [3] and will be described in what follows.

Cable modeling

Two-dimensional two-node isoparametric truss elements with large kinematics are used for cable modeling. Each cable element has four degrees of freedom corresponding to the horizontal and vertical translations at each end. A constant initial pre-strain corresponding to the installation conditions is prescribed as an initial condition for all cable elements. The mesh contains 100 cable elements in each span. Cable material properties are defined for tension only, assuming the absence of compression and small strain Hookian tension. The cable is assumed to be perfectly flexible in bending and torsion. The Young's moduli used in static and dynamic analyses are the same. Structural damping of the cable is modelled with equivalent viscous damping, while aerodynamic damping is not considered, due to its complexity. The values of viscous damping constants are calculated from the following equation:

$$C = 2\xi\sqrt{AEm} \tag{1}$$

where ξ is the damping ratio, A is the cross-section of the cable, E is the Young's modulus, and m is the mass per unit length of the cable or the cable-ice composition. The damping ratio was chosen as 2 % for the bare cable and 10 % for the iced cable following the recommendation in [3].

Modeling of suspension structure and insulator string

The suspension structure is modelled with a two-dimensional beam element having a rectangular cross-section. The beam is assumed to be perpendicular to the plane determined by the cable and the insulator string. Either end of the beam is fixed, while the insulator string is attached to the other end. The insulator string is also modelled with a two-dimensional beam element, and it is allowed to swing freely in the vertical plane. The cross-section of the insulator string is rectangular, but different from

that of a suspension structure. The catenary configuration of a two-span model with suspension structure between the spans and with fixed ends is shown in Figure 1.

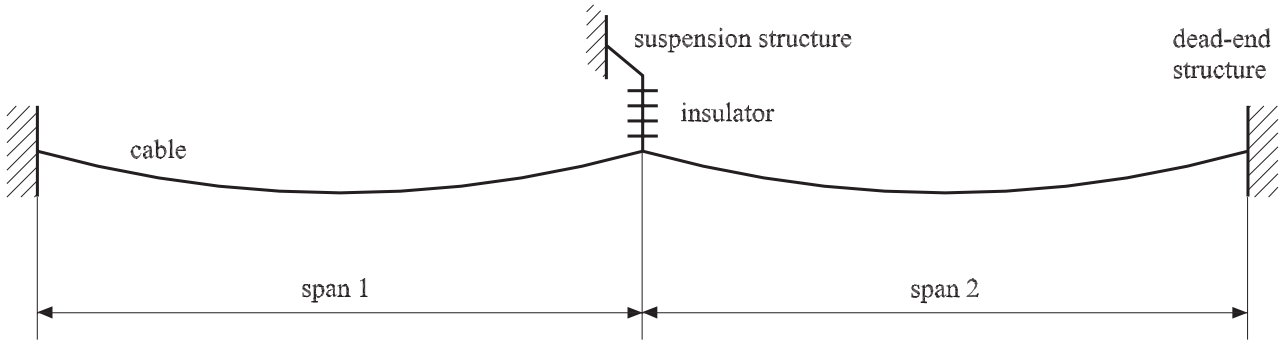

Figure 1: Catenary configuration of the two-span model

Ice modeling

The ice load is simulated by increasing the density of cable elements in the static analysis. Cable density of either span is suddenly decreased in the dynamic analysis when ice shedding occurs, while the density does not change in the span which remains loaded.

The density and other material properties of ice depend on the type of ice that accumulates on the cable. The types of ice and snow that may accrete on cables are rime ice, glaze ice, frost, dry snow and wet snow. Atmospheric conditions prevailing during the icing process determine what type of ice will form on the cable. In general, wet snow, rime ice and glaze ice appear most often on transmission lines, and glaze ice causes the highest ice load. The density of glaze ice approaches that of bubble-free ice, i.e. 917 kg/m^3. A density of 900 kg/m^3 is used in this study; it should be changed, however, when dynamics of cables loaded by different types of ice are examined.

The compressive stress-strain behavior of ice is greatly influenced by the strain rate [7]. The material exhibits macroscopically ductile behavior and the stress-strain curve is characterized by ascending and descending branches at low rates of deformation (below 10^{-4} – 10^{-3} 1/s). At higher rates, ice exhibits brittle behavior and the stress-strain curve is characterized by an ascending branch only. The strain rate often takes high values during the transient vibrations initiated by ice shedding on an adjacent span; it may sometimes exceed 10^{-2} 1/s. Thus, the ice exhibits brittle behavior, and breaks immediately after the stress in the ice exceeds its compressive strength. The tensile strength of ice is less than its compressive strength, and the ductile-brittle transition appears for lower strain rates [7-8]. The flexural strength of ice is also less than its compressive strength, and it does not depend significantly on the loading rate, at least for low rates of deformation [9].

In accordance with the above facts, two failure criteria are determined, as follows: Since the compressive strength of ice is greater than its tensile and flexural strengths, the compressive strength is used in the criteria that, thereby, provide sufficient conditions of fracture. These criteria are based on measured data reported in previous studies [10-11]. The authors of those papers determined the compressive strength and the corresponding critical strain for several values of the strain rate between 10^{-7} and 10^{-1} 1/s. The dependence of compressive strength on strain rate for a specific type of atmospheric ice was presented in [12], while the relationship of the tensile strength and strain rate for atmospheric ice was examined in [8]. They did not report, however, the critical value of strain where the maximum stress appears. Since stress is computed in our simulations by using the material properties of the cable, those results are not applicable for the ice. For these reasons, results of [10-11] are used in this study. Although these measurements were performed with bubble-free ice, they may serve as approximate values. The failure criteria are defined by the following equations:

$$\varepsilon_{cr1} = \begin{cases} 0.012 & \text{if } \log\dot{\varepsilon} \le -4.69 \\ 0.0005\log^2\dot{\varepsilon} + 0.0001 & \text{if } \log\dot{\varepsilon} > -4.69 \end{cases} \quad (2)$$

$$\varepsilon_{cr2} = 0.00017\log^2\dot{\varepsilon} + 0.00034\log\dot{\varepsilon} + 0.00027 \quad (3)$$

where $\dot{\varepsilon}$=dε/dt (1/s) is the strain rate, and ε (-) is the strain. Eq. (2) is fitted on the upper boundary of the data presented in [10] and [11], while Eq. (3) approximates the lower boundary of the same data as shown in Figure 2. Those data are obtained for different types of ice that were distinguished by grain size. Thus, Eq. (2) and Eq. (3) concern two types of ice with grain sizes of about 1.5 mm and about 5 mm, respectively, which represent ice with the greatest and the lowest strength examined in [10] and [11]. It should be noted that failure criteria must be improved in order to obtain reliable predictions of fracture of different types of atmospheric ice. Directions will be discussed later on.

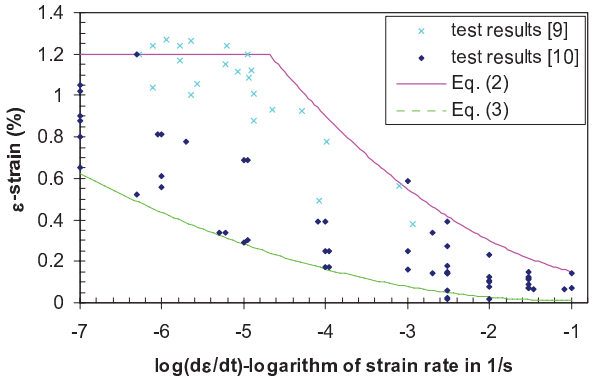

Figure 2: Strain at peak stress vs. strain rate, experimental data and failure criteria

The following methodology is applied in order to predict if ice breaking occurs: Dynamic analysis is carried out for 10 s after ice shedding takes place. This time interval is very short to reach the final steady state, but the highest strain rates are expected to arise at the beginning of transient vibrations. The strain and the strain rate are calculated at every time step in some elements of the cable-ice composition and they are saved in a database. These values are substituted into a failure criterion in a post-processing analysis. If the developing stress exceeds the compressive strength of ice (or the corresponding strain exceeds the critical strain) according to the failure criterion, then the post-processing analysis is interrupted and ice breaking is assumed in this moment.

COMPARISON OF SIMULATION RESULTS TO EXPERIMENTAL OBSERVATIONS

Simulation results will be compared to experimental observations reported in [1] in order to evaluate the reliability of the model. Measurements were performed on a five-span section of a transmission line. The central span was loaded, and the maximum jump height of the cable was determined after the sudden release of the ice load. The length of the central span was 247 m. The cable was made of copper-equivalent steel-cored aluminum; its geometrical and material data are given in Table 1. Three different suspension arrangements were used in [1]; the tests performed with standard suspension string of cap-and-pin insulators having a length of 2.1 m are simulated in this study. Further geometrical values of the insulator string and the suspension structure were not provided in the original paper, so approximate values are set in the simulations. The cross-section of the insulator and the suspension structure are 30 mm x 30 mm and 150 mm x 250 mm, respectively; while the length of the structure is 1 m. The material of both the insulator and the structure is assumed to be steel, so

material properties are chosen in accordance with this assumption, i.e. the Young's modulus is 200 GPa, Poisson's ratio is 0.3, and density is 7850 kg/m^3.

Two models are used to simulate some of the experiments presented in [1]. Both models include five spans, and the suspension structure described in the previous section is considered to be between adjacent spans. One of the models assumes fixed ends as shown in Figure 1, while the other model considers the same structures at the end points as between the spans. In reality, the dead-end structures of transmission lines are not rigid, but less flexible than the suspension structures; thus, their flexibility appears somewhere between the predictions of the two models. These models will be called Model-5R and Model-5F, in which the names refer to the number of spans and the rigid or flexible end points included in the model. Full portion of the central span was loaded in the experiments simulated, and four different loads were applied. Ice thicknesses and corresponding ice loads are presented in Table 2 for all four cases.

Simulations were carried out in two steps. First, the density of the middle span is increased due to ice load in the static analysis, and cable sag and cable tension at the mid-point of the span are calculated in the new configuration. Then, density is suddenly decreased at the beginning of dynamic analysis, and cable motion is simulated for 10 s. The maximum jump height and the maximum cable tension at the mid-point of the span during this time interval are determined from the time histories obtained.

Results of static analysis are evaluated by studying Figure 3. Measured data for the cable sag below the unloaded position in the loaded span are underestimated by about 25-30 % and about 20-25 % for Model-5R and Model-5F, respectively. The cable tension was not measured in [1], but they presented calculated values. The tension at the mid-point of the span as predicted by Model-5R is about 15 % greater than the values reported in [1], while Model-5F provides a 7-10 % overestimation of the same data. The overestimation of cable tension is a consequence of the underestimation of cable sag, because the increase of cable tension results in the decrease of cable sag. Results of dynamic analysis are presented in Figure 4. Both models provide very close approximation of the maximum jump height observed in the experiments for low loads, although they tend to overestimate it as the ice load increases: up to 12 % by Model-5R and up to 24 % by Model-5F. Maximum cable tensions occurring during vibration are in the range of cable tensions obtained in the static analysis. These values are not compared to experimental ones, since they were not reported in [1]. According to this evaluation, simulations provide satisfactory predictions, especially in the dynamic analysis. Discrepancies in the static analysis may arise from different sources. Lengths of the five spans were not exactly the same in the experiments, and suspension points did not appear at the same height at each tower. Moreover, some of the geometrical data were not presented in [1], which might also cause disagreement between simulation and experimental findings.

TABLE 1 – Parameters of the cable in Model-5R and in Model-5F

Cable diameter	(mm)	19.6
Cross-sectional area of the cable	(mm^2)	227.6
Weight per unit length of the cable	(N/m)	8.34
Cable density	(kg/m^3)	3734
Young's modulus of the cable	(GPa)	91.8
Sag of unloaded cable	(m)	5.18
Initial cable tension	(kN)	12.33

TABLE 2 – Load cases simulated by Model-5R and by Model-5F

Load #	1	2	3	4
Ice thickness (mm)	15.2	24.1	31.1	37.1
Ice load (N/m)	14.67	29.21	43.74	58.35

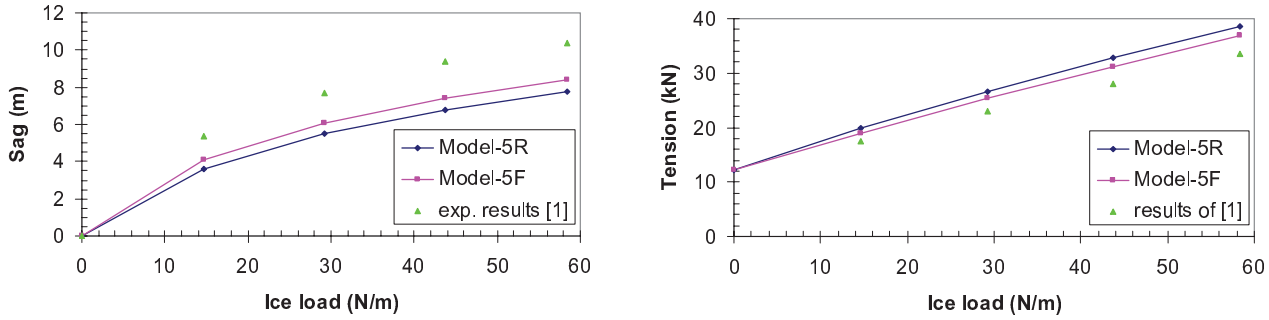

Figure 3: Cable sag below the unloaded position and cable tension at the mid-point of the span in static analysis

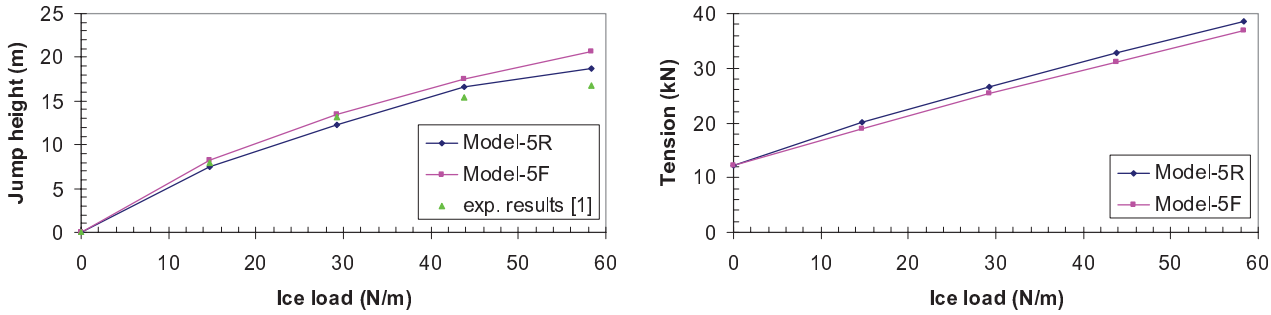

Figure 4: Maximum jump height and maximum cable tension at the mid-point of the span

MODELING THE DYNAMIC EFFECTS OF ICE SHEDDING ON A TWO-SPAN SECTION

Ice shedding and dynamic effects of the resulting vibrations on the ice and the suspension structure are modelled by applying the two-span model depicted in Figure 1. Ice sheds from either span, while the other span remains loaded during the simulations. Dead-ends are assumed to be rigid, so this model will be referred to as Model-2R. The suspension structure and insulator string between the spans have the same geometrical and material properties as introduced in the models of the previous section. The widely-used CONDOR conductor is modelled in these simulations, which is made of 54 aluminum alloy strands reinforced with a seven-wire steel core. The length of both spans is 200 m, and geometrical and material data of the cable are given in Table 3.

TABLE 3 – Parameters of the cable in Model-2R

Cable diameter	(mm)	27.8
Cross-sectional area of the cable	(mm^2)	455.1
Weight per unit length of the cable	(N/m)	14.9
Cable density	(kg/m^3)	3337
Young's modulus of the cable	(GPa)	68.3
Sag of unloaded cable	(m)	6.89
Initial cable tension	(kN)	10.93

TABLE 4 – Load cases simulated by Model-2R

Load #	1	2	3	4	5
Ice thickness (mm)	10	20	30	40	50
Ice load (N/m)	10.48	26.52	48.10	75.22	107.90
Sag below unloaded position (m)	0.24	0.57	0.97	1.40	1.86

Five load cases are examined in this set of simulations, among which the greatest one approaches the maximum ice load that is considered in the design of transmission lines. Ice thicknesses and corresponding ice loads in the five cases are presented in Table 4.
Simulations are carried out in two steps similarly to those presented in the previous section. Sags of the two spans are equal in the static analysis since the configuration is symmetric. Numerical values are provided in Table 4. Cable tensions obtained in the static analysis as well as the maximum cable tensions arising during vibration are presented in Figure 5. The values computed at the suspension point are shown in the figure since they were found greater than those acting in the middle of the span; they can also be compared to a failure criterion for the suspension structure, which was proposed in [13]. The author selected 100 kN as the longitudinal load at which a suspension structure fails. This condition is also shown in Figure 5, which predicts that the suspension structure will fail during the vibrations initiated by the shedding of 50 mm-thick ice.

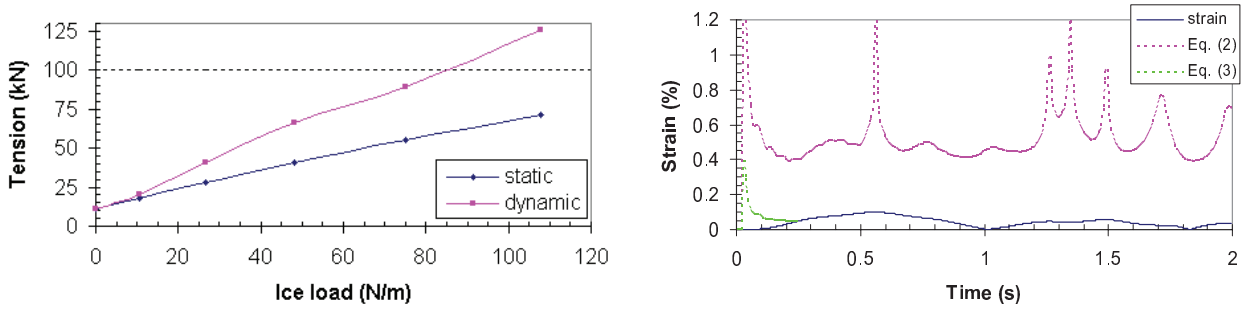

Figure 5: Maximum cable tension at the suspension point during the static and dynamic analyses, and time history of strain in the mid-point of the loaded span with failure criteria for load case #3

Strain and strain rate data obtained at the mid-point and at the suspension point of the loaded span are substituted into Eqs (2) and (3) in order to verify whether ice breaks during vibrations. Ice does not break according to the failure criterion represented by Eq. (2) even for the maximum ice load considered. If ice properties change, however, and the failure criterion defined by Eq. (3) is applied, then ice breaks when ice thickness is 30 mm or greater. The absolute value of strain is shown in Figure 5 as it varies in the first 2 s after ice shedding for load case #3, i.e. when ice thickness is 30 mm. Failure criteria are also determined in each step of computation and presented in the figure. It can clearly be seen that the strain is always significantly less than that determined by Eq. (2); it exceeds, however, the limit value given by Eq. (3) at 0.25 s. Thus, ice breaks in this moment and calculation is interrupted (the curve representing Eq. (3) is not continued). The results obtained show that vibrations initiated by ice shedding in the adjacent span may lead to ice failure, but they may also damage the suspension structure without breaking the ice. The outcome depends principally on the ice properties, which justifies making further efforts to consider different types of atmospheric ice in the model.

CONCLUSIONS AND RECOMMENDATIONS

A finite element model of iced cable and suspension structure of overhead transmission lines was applied to simulate vibrations as a result of shedding from one span of the line. Simulation results are compared to former experimental observations made on a five-span section. The study shows that the results of dynamic analysis are in satisfactory agreement with experimental data, and the maximum discrepancy regarding the results of static analyses does not exceed 25-30 % either. Further simulations are carried out with a two-span model. Five load cases and two criteria for ice failure are applied. One of these criteria concerns ice of small grain size, which type of ice does not break even during the most severe vibrations caused by shedding of the maximum ice load considered from the adjacent span. These vibrations lead, however, to the failure of the suspension structure, according to simulation results. The other criterion concerns ice of larger grain size, which type of ice breaks due to vibrations following the shedding of 30-mm thick or thicker ice load from the adjacent span.

The two simple criteria for ice failure that are applied in this paper are based on previous measurements performed to investigate the compressive strength of bubble-free ice. Atmospheric ice, however, is usually not bubble-free, and its tensile and flexural strengths are usually lower than its compressive strength. Therefore, improvements to the model regarding failure criteria are recommended as follows:

- include tensile strength and flexural strength of ice;
- specify ice properties depending on atmospheric conditions prevailing during ice accretion (further experimental observations would be beneficial);
- define a failure envelope that represents failure criterion under multiaxial loading, and;
- consider ice as a distinct material.

Acknowledgments

This research was carried out within the framework of the NSERC/Hydro-Québec Industrial Chair on Atmospheric Icing of Power Network Equipment (CIGELE) and the Canada Research Chair on Atmospheric Icing Engineering of Power Network (INGIVRE) at the University of Québec at Chicoutimi (UQAC). The authors would like to thank all the sponsors of the CIGELE for their financial support.

REFERENCES

[1] V. T. Morgan, D. A. Swift, 1964, "Jump height of overhead-line conductors after the sudden release of ice loads", *Proceedings of IEE,* vol. 111, no. 10, 1736-1746.

[2] A. Jamaleddine, G. McClure, J. Rousselet, R. Beauchemin, 1993, "Simulation of Ice Shedding on Electrical Transmission Lines Using ADINA", *Computers & Structures*, vol. 47, no. 4/5, 523-536.

[3] M. Roshan Fekr, G. McClure, 1998, "Numerical modelling of the dynamic response of ice shedding on electrical transmission lines", *Atmospheric Research,* vol. 46, 1-11.

[4] M. Roshan Fekr, G. McClure, D. Hartmann, 1998, "Investigation of Transmission Line Failure Due to Ice Shedding Using Dynamic Analysis", *Proceedings of the Eighth International Workshop on Atmospheric Icing of Structures,* Reykjavik, Iceland, 11-16.

[5] T. Kálmán, G. McClure, M. Farzaneh, L. E. Kollár, A. Leblond, 2005, "Dynamic Behavior of Iced Overhead Cables Subjected to Mechanical Shocks", *Proceedings of the 6th International Symposium on Cable Dynamics"*, Charleston, SC, USA.

[6] ADINA R & D, 2003, *ADINA – Theory and Modeling Guide*, Watertown, MA, USA, Report ARD 03-7.

[7] E. M. Schulson, 2001, "Brittle failure of ice", *Engineering Fracture Mechanics*, vol. 68, 1839-1887.

[8] J. Druez, P. McComber, C. Tremblay, 1989, "Experimental Results on the Tensile Strength of Atmospheric Ice", *Transactions of the CSME*, vol. 13, no. 3, 59-64.

[9] G. W. Timco, R. M. W. Frederking, 1982, "Comparative Strengths of Fresh Water Ice", *Cold Regions Science and Technology*, vol. 6, 21-27.

[10] M. Mellor, D. M. Cole, 1982, "Deformation and Failure of Ice under Constant Stress or Constant Strain-Rate", *Cold Regions Science and Technology*, vol. 5, 201-219.

[11] D. M. Cole, 1987, "Strain-Rate and Grain-Size Effects in Ice", *J. of Glaciology*, vol. 33, no. 115, 274-280.

[12] J. Druez, D. D. Nguyen, Y. Lavoie, 1986, "Mechanical Properties of Atmospheric Ice", *Cold Regions Science and Technology*, vol. 13, 67-74.

[13] M. Lapointe, 2003, *Dynamic analysis of a power line subjected to longitudinal loads*, M.Sc. thesis, McGill University, Montreal, QC, Canada.